

Ionic Liquids

Size Matters! On the Way to Ionic Liquid Systems without Ion Pairing

Alexander Rupp,^[a, b] Nataliya Roznyatovskaya,^[c] Harald Scherer,^[a] Witali Beichel,^[a, b] Petra Klose,^[a] Carola Sturm,^[a] Anke Hoffmann,^[a] Jens Tübke,^[c] Thorsten Koslowski,^[d] and Ingo Krossing^{*[a, b]}

Abstract: Several, partly new, ionic liquids (ILs) containing imidazolium and ammonium cations as well as the medium-sized [NTf₂]⁻ (0.230 nm³; Tf=CF₃SO₃⁻) and the large [Al(hfip)₄]⁻ (0.581 nm³; hfip=OC(H)(CF₃)₂) anions were synthesized and characterized. Their temperature-dependent viscosities and conductivities between 25 and 80 °C showed typical Vogel–Fulcher–Tammann (VFT) behavior. Ion-specific self-diffusion constants were measured at room temperature by pulsed-gradient stimulated-echo (PGSTE) NMR experiments. In general, self-diffusion constants of both cations and anions in [Al(hfip)₄]⁻-based ILs were higher than in [NTf₂]⁻-based ILs. Ionicities were calculated from self-diffusion constants and measured bulk conductivities, and

showed that [Al(hfip)₄]⁻-based ILs yield higher ionicities than their [NTf₂]⁻ analogues, the former of which reach values of virtually 100% in some cases. From these observations it was concluded that [Al(hfip)₄]⁻-based ILs come close to systems without any interactions, and this hypothesis is underlined with a Hirshfeld analysis. Additionally, a robust, modified Marcus theory quantitatively accounted for the differences between the two anions and yielded a minimum of the activation energy for ion movement at an anion diameter of slightly greater than 1 nm, which fits almost perfectly the size of [Al(hfip)₄]⁻. Shallow Coulomb potential wells are responsible for the high mobility of ILs with such anions.

Introduction

Ionic liquids (ILs) are classically defined as salts that melt below 100 °C. Room-temperature ILs (RTILs) accordingly melt below 25 °C. Selected ILs may have characteristics that are not found in this combination elsewhere, namely, relatively high conductivities, low viscosities, negligible vapor pressures, low flammability, high electrochemical resistance, good gas-storage capability, and often low toxicity.^[1,2] The potential of combining several of those properties in one IL makes them interest-

ing for various applications, for example, as electrolytes, as polar solvents and reaction media, and for fundamental research.^[3–17] For example, an ideal IL electrolyte for (electrochemical) energy-conversion and energy-storage devices would show low viscosity, high conductivity and self-diffusion constants, a very low melting point, and a large electrochemical stability window. ILs with both anions of this study fulfill these requirements.

The quantities of these dynamic or transport properties of ILs are interconnected by several relations. First, self-diffusion constants D and viscosities η are related by the Stokes–Einstein equation^[18] [Eq. (1)],

$$D = \frac{kT}{c\pi\eta r} \quad (1)$$

where k is the Boltzmann constant, T the absolute temperature, c a constant between 4 and 6, and r the radius.

It is still under debate whether the Stokes–Einstein equation can be applied to IL systems, but due to its simplicity it is often used to describe ILs.^[19,20] Second, a relation between conductivities σ and self-diffusion constants is given by the Nernst–Einstein equation [Eq. (2)],

$$\sigma = \frac{z^2 e^2 \rho N_A}{MkT} \cdot D \quad (2)$$

[a] Dipl.-Chem. A. Rupp, Dr. H. Scherer, Dr. W. Beichel, P. Klose, C. Sturm, Dr. A. Hoffmann, Prof. Dr. I. Krossing
Albert-Ludwigs-Universität Freiburg
Institut für Anorganische und Analytische Chemie
Albertstrasse 21, 79104 Freiburg (Germany)
E-mail: ingo.krossing@ac.uni-freiburg.de

[b] Dipl.-Chem. A. Rupp, Dr. W. Beichel, Prof. Dr. I. Krossing
Freiburger Materialforschungszentrum
Stefan-Meier-Strasse 21
79104 Freiburg (Germany)

[c] Dr. N. Roznyatovskaya, Dr. J. Tübke
Fraunhofer-Institut für Chemische Technologie
Angewandte Elektrochemie
Joseph-von-Fraunhofer-Strasse 7, 76327 Pfinztal (Germany)

[d] Prof. Dr. T. Koslowski
Albert-Ludwigs-Universität Freiburg
Institut für Physikalische Chemie
Albertstrasse 23a, 79104 Freiburg (Germany)

Supporting information for this article is available on the WWW under <http://dx.doi.org/10.1002/chem.201400168>.

where z is the charge, e the elementary charge, ρ the density, N_A the Avogadro constant, and M the molecular mass.

Third, viscosities η and molar conductivities λ are connected by Walden's rule^[21,22] [Eq. (3)], which results from Equations (1) and (2) and is commonly accepted to be valid also for ILs.^[5]

$$\lambda\eta = \text{const.} \quad (3)$$

One drawback of all of these often-used models is that some of their initial assumptions are not valid in the case of pure ILs: Walden's rule was developed for dilute solutions, the Stokes–Einstein equation was derived for a single particle diffusing in a homogeneous solvent, and self-diffusion constants in the Nernst–Einstein equation are those at infinite dilution. Admittedly, in most cases the adequate results that one obtains when using these relations are a sufficiently good argument for their application.

For the quantitative description of temperature-dependent viscosities of ILs, it has been shown by many groups that data fitting with a Vogel–Fulcher–Tammann (VFT) ansatz [Eq. (4)] yields excellent results,^[23–26]

$$\eta = \eta_0 \exp\left(\frac{B}{T - T_0}\right) \quad (4)$$

where η_0 is the viscosity at infinite temperature, B a constant, and T_0 the Vogel temperature.

In the case of conductivities of ILs, also an Arrhenius approach [Eq. (5)] is applicable, yet VFT fits [Eq. (6)] exhibit higher accuracy,

$$\sigma = \sigma_0 \exp\left(-\frac{A}{RT}\right) \quad (5)$$

$$\sigma = \sigma_0 \exp\left(-\frac{B}{T - T_0}\right) \quad (6)$$

where σ_0 is the conductivity at infinite temperature, A the activation energy, B a constant, and T_0 the Vogel temperature.

By combining self-diffusion and conductivity measurements, one can assess the so-called ionicities [Eq. (7)],^[27] which give quantitative information about the degree of ion pairing within the IL,

$$I = \frac{\sigma_{\text{exp}}}{\sigma_{\text{diff}}} = \frac{\sigma_{\text{exp}} M k T}{e^2 \rho N_A (D^+ + D^-)} \quad (7)$$

where σ_{exp} is the experimentally measured conductivity and σ_{diff} the conductivity calculated from the measured self-diffusion constants.

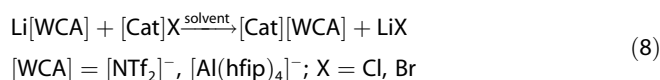
Herein, we present viscosity, conductivity, self-diffusion, and ionicity data for 24 ILs, seven of which were synthesized for the first time. Our results show that introduction of the large $[\text{Al}(\text{hfp})_4]^-$ anion ($\text{hfp} = \text{OC}(\text{H})(\text{CF}_3)_2$), which is an even more

weakly coordinating anion than the medium-sized $[\text{NTf}_2]^-$ anion ($\text{Tf} = \text{CF}_3\text{SO}_2$), shifts the IL systems towards an increasingly ideal behavior that is governed by ion size (i.e., molecular volumes) rather than by ion surface (i.e., intermolecular interactions). These experimental findings were supported by a modified Marcus-theory ansatz.

Results and Discussion

Syntheses and characterization

A set of 24 ILs (full list in Supporting Information, abbreviations in Appendix) was prepared or, where possible, purchased. The syntheses were carried out by anion metathesis [Eq. (8)] according to reported procedures.^[4,28,29]



All ILs were fully characterized by IR, Raman, and NMR spectroscopy (^1H , ^{19}F and ^{27}Al). Purity was additionally always checked by ^7Li NMR spectroscopy, to ensure the absence of lithium halides. In the case of $[\text{Al}(\text{hfp})_4]^-$ -based ILs, due to the known decomposition pathway of the hfp group,^[3] complete removal of H_2O in vacuum always results in formation of impurities in the ^{19}F NMR spectra. We had to find a balance between low H_2O contents (<200 ppm) and ^{19}F NMR spectra showing anion impurities, probably resulting from the formation of the $[\text{FAl}(\text{hfp})_3]^-$ anion^[3] in amounts of at most 3%, which, in our experience, does not alter the properties of $[\text{Al}(\text{hfp})_4]^-$ ILs by more than 2%. The $[\text{NTf}_2]^-$ -based ILs were dried at $90^\circ\text{C}/10^{-3}$ mbar until water contents of <20 ppm were achieved (Karl–Fischer titration). Full characterization details are deposited in the Supporting Information.

Viscosity and conductivity measurements

The temperature-dependent viscosities and conductivities of all 24 ILs were determined between room temperature and 80°C during heating in their liquid range, and fitting of the data with a VFT ansatz was done subsequently. The results are shown in Figures 1 and 2, respectively, while the fit parameters are given in Tables 5 and 6 in the Appendix. All fits show R^2 values greater than or equal to 0.999, and both viscosities and conductivities are in accordance with expected results. A more detailed description of these results can be found in the Appendix.

Figures 1 and 2 show that $[\text{Al}(\text{hfp})_4]^-$ -based ILs almost always show viscosities equal to or lower than and conductivities equal to or higher than those of $[\text{NTf}_2]^-$ -based ILs, the only exceptions being $[\text{C}_2\text{MIm}]^+$, $[\text{AllylMIm}]^+$, $[\text{C}_4\text{MIm}]^+$, and $[\text{N}_{1123}]^+$ salts. Clearly, the nature of the cations also has an influence on the properties: exchanging imidazolium ions against ammonium ions results in an approximately tenfold increase in viscosity. Additionally, the properties of $[\text{Al}(\text{hfp})_4]^-$ -based ILs depend much less on the cation compared to their $[\text{NTf}_2]^-$ analogues.

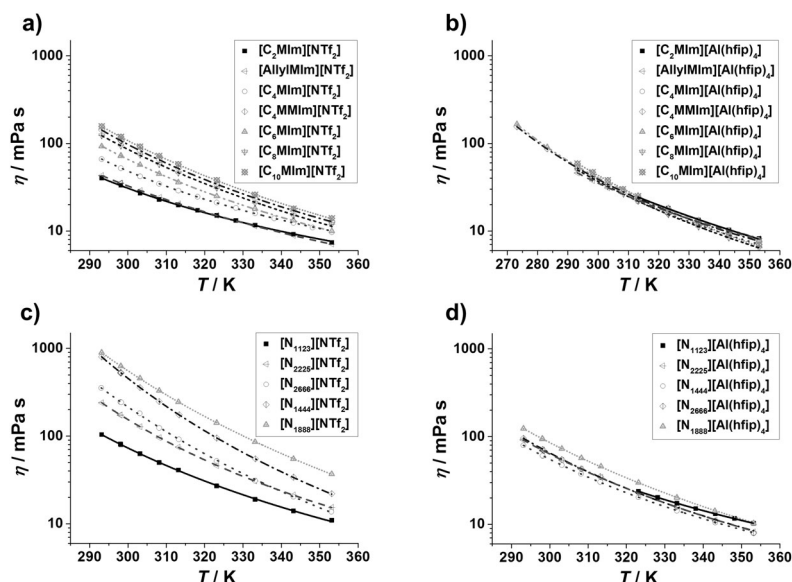


Figure 1. Viscosity data of all 24 investigated ILs. Viscosities were measured in the liquid range of the ILs from 25 to 80 °C.

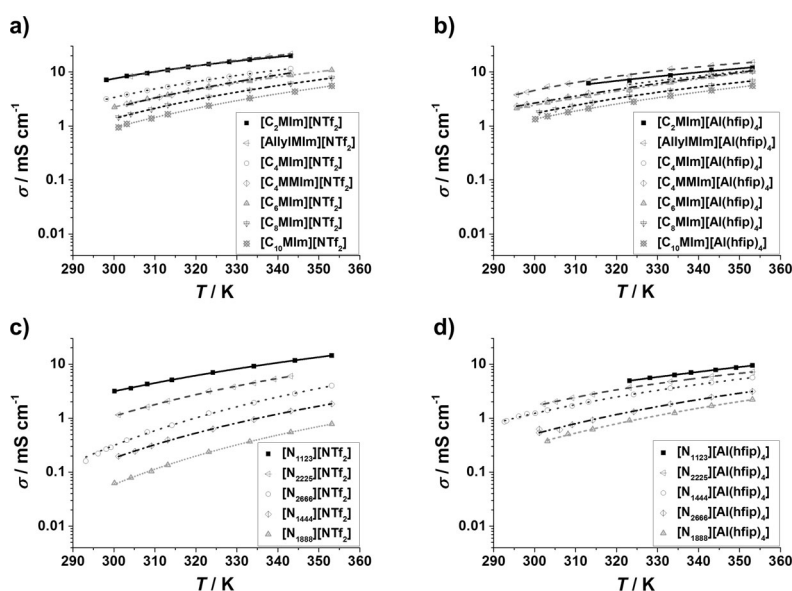


Figure 2. Conductivity data of all 24 investigated ILs. Conductivities were measured in the liquid range of the ILs from room temperature to 80 °C.

This feature can be explained by the different properties of the two anions: $[\text{Al}(\text{hfip})_4]^-$ is a large and spherical ion with an almost completely fluorinated and thus hardly polarizable surface. Interactions with other nearby ions will therefore be weak, nondirectional, and independent of the structure of the other ion. Metaphorically speaking, cations are moving through a more or less noninteracting network of anions that governs the overall properties. $[\text{NTf}_2]^-$ ions, on the other hand, are to a certain extent able to interact through their more Lewis-basic N and O atoms. These interactions are dependent on the cation structure. Aggregation is typically favored in ILs

with longer alkyl chains ($n > 6$), apparently due to the increasing importance of dispersive interactions in these more polarizable groups.

Comparison of the different sets of ILs (Figure 1) shows the expected tendency of ILs with larger cations to have higher viscosities due to more hindered migration. This becomes even clearer when one considers that the migration of ions in ILs can be described by a hole theory.^[30] Despite the much larger molecular volume of $[\text{Al}(\text{hfip})_4]^-$ (0.581 nm³) compared to $[\text{NTf}_2]^-$ (0.233 nm³),^[31,32] both $[\text{C}_n\text{Mim}][\text{NTf}_2]$ and $[\text{NR}_n][\text{NTf}_2]$ ILs are typically equally or even more viscous than their $[\text{Al}(\text{hfip})_4]^-$ analogues. The only exceptions to this behavior are ILs with the very small $[\text{C}_2\text{Mim}]^+$ ($V^+ = 0.156 \text{ nm}^3$)^[31,32] and $[\text{N}_{1123}]^+$ ($V^+ = 0.180 \text{ nm}^3$)^[31,32] cations.

This unexpected behavior gave first hints that ILs with a large and very weakly coordinating anion exhibit almost ideal and undisturbed physical properties. The volume of $[\text{Al}(\text{hfip})_4]^-$ compared to that of $[\text{NTf}_2]^-$ suggested that ion pairing should at least be strongly subdued to allow for the high conductivities and low viscosities of $[\text{Al}(\text{hfip})_4]^-$ ILs. To shed further light on this idea, a complete set of diffusion measurements was done by NMR methods.

Pulsed-gradient stimulated-echo (PGSTE) NMR measurements of self-diffusion constants

Ion-specific self-diffusion constants of all RTILs within the set of ILs were measured with PGSTE-NMR experiments at room temperature. Cation diffusion constants D^+ were extracted from ¹H spectra; anion diffusion constants D^- were extracted from both ¹⁹F and ¹H spectra, unless the anion signal could not be separated properly from all cation signals. Both nuclei of each IL were measured at least twice. Fitting was done with the Stejskal–Tanner equation^[33] [Eq. (9)] by using the integrals of the NMR signals. The values given in Table 1 are arithmetic means of these measurements. The total error including tem-

Table 1. Ion-specific diffusion constants of the measured RTILs. Molecular volumes were obtained through DFT calculations; the calculation protocol can be found elsewhere.^[31] Diffusion constants $D^{+/-}$ were obtained by signal integration.

Cation	V_m^+ [nm ³]	D^+ [10 ⁻¹¹ m ² s ⁻¹]		D^- [10 ⁻¹¹ m ² s ⁻¹]	
		[NTf ₂] ⁻	[Al(hfip) ₄] ⁻	[NTf ₂] ⁻	[Al(hfip) ₄] ⁻
[C ₂ MIm] ⁺	0.156	4.31	(1.94) ^[a]	2.64	(0.797) ^[a]
[AllylMIm] ⁺	0.168	4.46	4.77	2.90	1.89
[C ₄ MIm] ⁺	0.197	2.37	2.20 ^[a]	1.70	1.30 ^[a]
[C ₄ MMIm] ⁺	0.218	1.33	2.78	0.97	1.69
[C ₆ MIm] ⁺	0.244	1.38	2.80	1.23	1.80
[C ₈ MIm] ⁺	0.288	0.895	2.01	1.43	1.46
[C ₁₀ MIm] ⁺	0.331	0.695	1.60	0.792	1.29
[N ₁₁₂₃] ⁺	0.180	1.35	not an RTIL	1.11	not an RTIL
[N ₁₄₄₄] ⁺	0.322	0.343	1.21	0.153	0.966
[N ₁₈₈₈] ⁺	0.604	0.105	0.633	too viscous	0.747
[N ₂₂₂₅] ⁺	0.268	0.520	2.10	0.512	1.50
[N ₂₆₆₆] ⁺	0.484	0.149	0.725	0.181	0.757

[a] [C₂MIm][Al(hfip)₄]⁻ and [C₄MIm][Al(hfip)₄]⁻ are not RTILs either, yet they could be supercooled and measured at room temperature.

perature fluctuations was estimated by repeated measurements and comparison to literature data^[34-41] to be 5–10%.

$$\frac{I(\delta, \Delta, g)}{I(\delta, \Delta, g=0)} = \exp\left[-\gamma^2 \delta^2 g^2 D \left(\Delta - \frac{\delta}{3}\right)\right] \quad (9)$$

In Equation (9), $I(\delta, \Delta, g)$ is the signal intensity with applied gradient of strength g , $I(\delta, \Delta, g=0)$ the signal intensity without gradient g , γ the gyromagnetic ratio, δ the duration of the gradient pulse, and Δ the diffusion delay.

From Table 1 it is obvious that self-diffusion constants decrease with increasing cation size. However, the decrease seems to be more pronounced for the cations than for the anions, as the difference between D^+ and D^- also decreases. For example, in [C₂MIm][NTf₂]⁻ the cation is nearly twice as fast as the anion, whereas in [C₁₀MIm][NTf₂]⁻, the two ions diffuse almost equally fast. Furthermore, ammonium-based ILs tend to diffuse more slowly than imidazolium ILs of comparable ion size. Figure 3 shows the relation of cation size and ion diffusion constants for all sets of ILs.

In contradiction to common expectations, almost all cations diffuse faster when they are combined with the larger anion [Al(hfip)₄]⁻. Although [C₂MIm][Al(hfip)₄]⁻ and [C₄MIm][Al(hfip)₄]⁻ are not really RTILs, they could be

supercooled for several measurements. Even more striking is that the anion self-diffusion constants of [Al(hfip)₄]⁻ usually exceed those of the corresponding [NTf₂]⁻ ILs. Typically, larger particles move more slowly due to steric hindrance, increased interaction with their surroundings, and their typically higher molecular mass (cf. M_r ([Al(hfip)₄]⁻) = 695.10, M_r ([NTf₂]⁻) = 280.15). Figure 3c and d reveal another important feature: In these plots, the ratio of cation and anion self-diffusion constants of [NTf₂]⁻ and [Al(hfip)₄]⁻ ILs, respectively, were plotted versus the molecular volume of the cations, and a fit was done by utilizing a generalized form of the Stokes–Einstein equation [Eq. (1)]. The justification for this model is as follows: The constant c in Equation (1) originally represented the conditions of the diffusion process (sticky or slip conditions). From our measurements, neither the value of c can be derived nor can it be said whether the c values are the same for cations and anions of one IL. To avoid this problem, we evaluated the ratio of cationic and anionic diffusion constants, yielding the first part of Equation (10). In most ILs, the ions are far from spherical. Therefore, the radius is not very suitable for this study and is replaced by the third root of the molecular volume V_m . Also, $c^{+/-}$ values are combined to yield a new parameter A^* . This results in the right part of Equation (10).

$$\frac{D^+}{D^-} = \frac{c^- r^-}{c^+ r^+} = A^* \left(\frac{V_m^-}{V_m^+}\right)^{1/3} \quad (10)$$

Since in Figure 3c and d, the respective anions remain constant, we combine A^* and $(V_m^-)^{1/3}$ to get a new parameter A . Additionally, since we cannot be sure whether the Stokes–Ein-

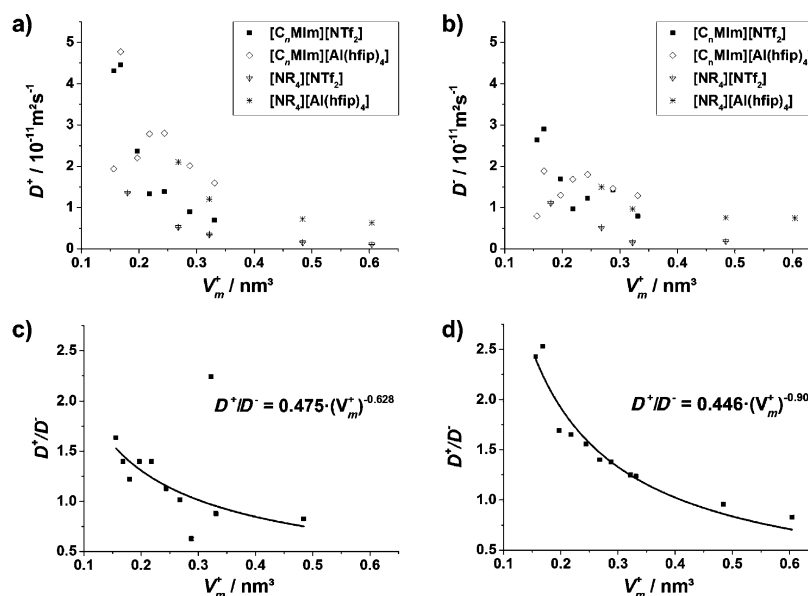


Figure 3. Results of the PGSTE NMR measurements. a) Comparison of cation self-diffusion constants of [NTf₂]⁻ and [Al(hfip)₄]⁻ ILs with respect to the cation volume. b) Comparison of anion self-diffusion constants of [NTf₂]⁻ and [Al(hfip)₄]⁻ ILs with respect to the cation volume. c) Combined fit of the ratios of the diffusion constants of all investigated [NTf₂]⁻ ILs. The fitting function was a generalized Stokes–Einstein ansatz of the form $y = ax^{-b}$ without considering [N₁₄₄₄][NTf₂]⁻ and [C₈MIm][NTf₂]⁻. d) Corresponding fit of all investigated [Al(hfip)₄]⁻ ILs.

stein equation is valid in our case, the exponent is not necessarily 1/3, and we replace it by a second parameter b . Hence, our final equation is Equation (11).

$$\frac{D^+}{D^-} = A(V_m^+)^{-b} \quad (11)$$

If Equation (1) were valid, one would expect the ratios to show a behavior of the form $y = Ax^{-1/3}$, even when different c factors for cations and anions are considered. However, neither $[\text{NTf}_2]^-$ nor $[\text{Al}(\text{hfp})_4]^-$ ILs show such behavior. Whereas their pre-exponential factors are very similar, they differ in the exponents, which are 0.63 and 0.91, respectively (see Figure 3c and d). Note that in the case of $[\text{NTf}_2]^-$ ILs, fitting was done without considering the values of $[\text{N}_{1444}][\text{NTf}_2]$ and $[\text{C}_8\text{MIm}][\text{NTf}_2]$. The former—like $[\text{N}_{1888}][\text{NTf}_2]$ —was hardly measurable due to its high viscosity and the resulting noncorrectable phase errors. The latter has an unusually low ratio, but it is not clear where this effect stems from, and we omitted this value.

Experimental self-diffusion constants also allow for the calculation of viscosities through the Stokes–Einstein equation. The results of these calculations are deposited in the Supporting Information. However, no general trend could be observed, except for a tendency that viscosities are underestimated by these calculations in the case of $[\text{NTf}_2]^-$ ILs and rather overestimated in the case of $[\text{Al}(\text{hfp})_4]^-$ ILs. In summary, our analysis of the PGSTE measurements, in accordance with literature data,^[19] emphasizes that hydrodynamic models may only be used with much caution, since they might not—or at least not always—apply for ILs.

Ionicities

By dividing the experimentally measured conductivities σ_{exp} by the conductivities calculated from the measured self-diffusion constants σ_{diff} , it is possible to calculate the so-called ionicities.^[27,39] These can be seen as a parameter to describe the degree of ion pairing in ILs. The basic assumptions for this theory are that, in PGSTE-NMR experiments, the detected diffusion is an average of all species containing the investigated ions in solution. Ion pairs may exist but are normally too short-lived to give rise to individual signals in the NMR spectrum. Therefore, conductivities calculated from those diffusion constants should be an upper limit, presuming that all ions contribute to conductivity (=ideal limiting conductivity). The real ideal conductivity can, however, not be measured, because the measured diffusion constants are the mean of the diffusion constants of unpaired and (slower) paired ions. Thus, σ_{diff} is close to but does not equal the ideal conductivity. Nevertheless, it is a good and easily accessible reference value and allows for a quantitative comparison of degrees of ion pairing. During bulk conductivity measurements, only net charged particles can contribute to conductivity. Ion pairs decrease the number of available charge carriers and thus limit the detected conductivity to an often much lower value. As a result, the absence of ion pairing would yield ionicities of 1.0 or 100%, and complete ion pairing results in ionicities of 0.0 or 0%. The ionicities

of a small number of $[\text{NTf}_2]^-$ ILs are known to be 0.5–0.8.^[27] This means that even in the very best $[\text{NTf}_2]^-$ IL, namely, the low-viscosity, highly conducting $[\text{C}_2\text{MIm}][\text{NTf}_2]$, 20% of the ions are not available for charge transport, which is an annoying feature especially for electrochemical applications. Before we discuss the ionicity data, we note that the Nernst–Einstein equation, which is used to calculate conductivities from self-diffusion constants, may still be valid even if the Stokes–Einstein equation does not apply in the examined systems. Also, its successful application in IL research shows that it yields empirically good results,^[25,42,43] whereas the Stokes–Einstein relation clearly failed here.

Table 2 lists ionicity data of all measured ILs. The estimated overall error of the ionicities is about 10%. The values show that $[\text{Al}(\text{hfp})_4]^-$ ILs not only show higher conductivities and dif-

Table 2. Ionicities of all measured RTILs.

Cation	Anion	
	$[\text{NTf}_2]^-$	$[\text{Al}(\text{hfp})_4]^-$
$[\text{C}_2\text{MIm}]^+$	0.67 (0.75) ^[a]	[2.10]
$[\text{AllylMIm}]^+$	0.62	0.87
$[\text{C}_4\text{MIm}]^+$	0.56 (0.61) ^[a]	1.03
$[\text{C}_4\text{MMIm}]^+$	0.66	0.83
$[\text{C}_6\text{MIm}]^+$	0.63 (0.57) ^[a]	0.73
$[\text{C}_8\text{MIm}]^+$	0.48 (0.54) ^[a]	0.82
$[\text{C}_{10}\text{MIm}]^+$	0.55	0.79
$[\text{N}_{1123}]^+$	0.82	no D^+ , D^-
$[\text{N}_{1444}]^+$	0.50	0.87
$[\text{N}_{1888}]^+$	no D^-	0.47
$[\text{N}_{2225}]^+$	0.95	0.69
$[\text{N}_{2666}]^+$	0.74	0.80

[a] Data given in parentheses for comparison stem from the work of Watanabe et al.^[27]

fusion constants, but also particularly high ionicities, typically 10–40% higher than those of $[\text{NTf}_2]^-$ ILs with the same cations. To the best of our knowledge, this is the first time that ILs with ionicities of up to 100% have been reported. However, an IL system completely without any interaction is not possible. In this light, ion pairs may also exist in the best $[\text{Al}(\text{hfp})_4]^-$ ILs, but are clearly less favored than in $[\text{NTf}_2]^-$ ILs. This is in agreement with dielectric spectroscopy, which indicated the absence of ion pairing in $[\text{Al}(\text{hfp})_4]^-$ ILs down to the very short picosecond range.^[19] The unusually high ionicity of $[\text{C}_2\text{MIm}][\text{Al}(\text{hfp})_4]$ can be attributed to subdiffusion in the supercooled melt and a resulting underestimation of σ_{diff} .

The effect of the cation on ionicities can also be seen. Dispersion forces, steric effects, strength of Coulomb forces, and interaction with anions differ from cation to cation. As a result, the effect of the cation apparently is not negligible and can lead to extraordinarily high ($[\text{C}_4\text{MIm}][\text{Al}(\text{hfp})_4]$) or just moderate ionicities ($[\text{C}_4\text{MIm}][\text{NTf}_2]$). Going from $[\text{C}_4\text{MIm}][\text{Al}(\text{hfp})_4]$ to ILs with only slightly larger imidazolium cations supports this finding with approximately 20% lower ionicities.

Discussion of the unusually low viscosities, high conductivities, high self-diffusion constants, and high ionicities of [Al(hfip)₄]⁻ ILs

The viscosity data show two things: imidazolium ILs are less viscous than ammonium ILs, and [Al(hfip)₄]⁻ ILs are equally or less viscous than [NTf₂]⁻ ILs. Flat imidazolium ions only limit ion movement in two dimensions and thus yield ILs of lower viscosity than spherical ammonium ions.^[44,45] The lower viscosities of [Al(hfip)₄]⁻ ILs can be explained by weaker interactions in these ILs because of the more weakly coordinating nature of [Al(hfip)₄]⁻.^[4] Additionally, hydrogen-bond networks can lead to a flattening of the energy landscape and thereby increase ion mobility and dynamic properties.^[46–48] Similar trends and conclusions apply for conductivities. The higher conductivities of ILs with small cations can be attributed to the higher charge-carrier densities and, of course, to the lower viscosities, which ease ion transport. Altogether, the conductivity results resemble the viscosity measurements: less interaction, combined with a network of hydrogen bonds if possible, improves transport properties of ILs.

Self-diffusion constants of [Al(hfip)₄]⁻-based ILs generally are higher than those of corresponding [NTf₂]⁻ ILs. The [Al(hfip)₄]⁻ anion, which is covered with an almost completely fluorinated and thus nonpolarizable surface and has a much larger surface area, has weaker coordinating characteristics than [NTf₂]⁻. Consequently, all mentioned dynamic properties crucially rely on the ability of particles to change their position as easily as possible. Every joule of attractive forces, resulting for instance from Coulomb or dispersive interactions, limits viscosities, conductivities, and self-diffusion constants. Especially Coulomb interactions should be limited in [Al(hfip)₄]⁻ ILs because of the reciprocal dependence of the Coulomb potential E_C on the radius r [Eq. (12)],

$$E_C = \frac{q_1 q_2}{4\pi\epsilon_0 r} \quad (12)$$

where q_1 and q_2 are the electric charges of two interacting particles, ϵ_0 is the vacuum permittivity and r the distance between the particles.

The fit of D^+/D^- versus V_m^+ (Figure 3) can give even more insight into the intermolecular forces. We propose that the exponents b [cf. Eq. (11)] are related to the degree of interactions within the ILs. If no other interactions are present, only the size of the ions determines the three-dimensional Coulomb potential of the IL that limits mass transport. Therefore, a volume-dependent term, that is, an exponent of unity should appear in this representation. If surface-dependent interactions occur, the exponent should also reduce to a surface term, or $V^{-2/3}$ if the contributions of these interactions are dominant. In the light of these assumptions, three main conclusions can be drawn for the applicability of the Stokes-Einstein equation for IL systems:

- 1) The Stokes–Einstein equation qualitatively describes the results correctly with ratios of the cation and anion diffusion constants that decrease with increasing cation size.
- 2) It fails in the quantitative description of the results. Trying to fit the data to an exponent of $b = 1/3$ yields R^2 values of < 0.7 . This is not surprising, as the requirements for its application are at least not entirely fulfilled: The “solvent”, for example, does not consist of a homogeneous medium.
- 3) [Al(hfip)₄]⁻ ILs show a more ideal behavior with an exponent closer to unity. [NTf₂]⁻ ILs, on the other hand, have a dependence on the cation molecular volume that is more governed by additional surface-based, likely dispersive interactions. This becomes manifest in a b value of roughly $2/3$.

The ionicity data underline the hypothesis that reduced interactions are responsible for the good performance of [Al(hfip)₄]⁻ ILs as possible electrolytes. Due to this reduction, not only is the movement of ions facilitated, but also the formation of ion pairs is inhibited. Consequently, more ions are available to take part in dynamic processes. Our results imply that systems almost without ion pairing are possible and can be a starting point for the synthesis of better systems for applications in which ILs with as many free ions as possible are needed, for instance, in electrolyte research.

To support this hypothesis, one can examine qualitatively the energy barriers that lie between two hole positions of a moving ion inside the IL. Figure 4 shows the difference be-

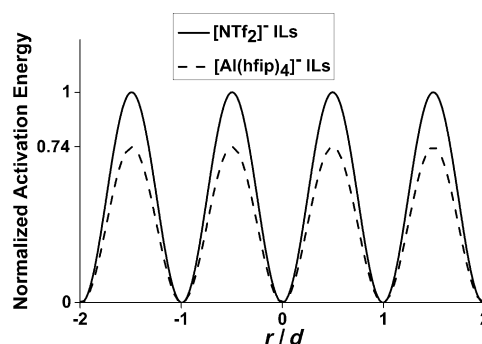


Figure 4. Energy profiles of the ions diffusing in an IL. The abscissa shows the normalized ion positions in multiples of the distance r from the lowest-energy equilibrium position, in relation to the average distance d from one equilibrium position to an adjacent equilibrium position.

tween [Al(hfip)₄]⁻ and [NTf₂]⁻ ILs. Assuming that the total interaction energy E_T in an IL is mainly determined by the additive terms of Coulomb (E_C) and dispersion energies (E_D), $E_T = E_C + E_D$, the energy barrier for diffusion of cations in [Al(hfip)₄]⁻ ILs should roughly be only 74% of that of the cations in [NTf₂]⁻ ILs. This simplified value results from the differences in the molecular volumes of the IL anions and the assumption that the majority of E_T is governed by E_C .

Of course, dispersion still can have an effect, but a smaller one compared to the effect of Coulomb interactions. However, on extending the alkyl-chain lengths of the imidazolium cat-

ions, dispersion increases, which ultimately leads to an increase in intermolecular forces and thereby decreased ionicities. This is in complete agreement with all experimental data collected in Figures 1 and 2 as well as Tables 1 and 2.

When an anion is moving from one minimum position to an adjacent minimum position, it must pass through a transition state in which its energy is raised. In the case of the large $[\text{Al}(\text{hfp})_4]^-$ anion, repulsive Coulomb interactions between anions during the motion are much weaker than for the smaller $[\text{NTf}_2]^-$ anion. Therefore, a larger anion, here further supported by a hardly polarizable surface that is formed mainly by aliphatic C–F bonds, enables easier ion movement in this case. This finding contradicts the common consideration that larger ions always lead to less favorable dynamics and transport properties. The limitations of this model are given by the nature of the anions. $[\text{Al}(\text{hfp})_4]^-$ not only shows weak interactions but also has a spherical shape, which isotropically distributes these interactions. In contrast, $[\text{NTf}_2]^-$ has a more cylindrical shape and thus shows more directional and less distributed interactions. These influences must be considered, otherwise comparison with ionicities of small, but spherical $[\text{PF}_6]^-$ ILs^[49] or even with large, but more coordinating anions with stronger directed or dispersive interactions can lead to errors.

To support this hypothesis and to get an at least semiquantitative insight into the differences between $[\text{NTf}_2]^-$ and $[\text{Al}(\text{hfp})_4]^-$, we exemplarily conducted a Hirshfeld analysis^[50–52] of the crystal structures of $[\text{C}_4\text{MIm}][\text{Al}(\text{hfp})_4]$ and $[\text{C}_4\text{MIm}][\text{NTf}_2]$. Table 3 lists the results for contacts between H and F and between H and O, respectively.

Table 3. Hirshfeld analysis of $[\text{C}_4\text{MIm}][\text{Al}(\text{hfp})_4]$ and $[\text{C}_4\text{MIm}][\text{NTf}_2]$.		
$[\text{C}_4\text{MIm}][\text{Al}(\text{hfp})_4]$	H–F [%]	H–O [%]
cation	80.6	5.3
anion	50.0	2.9
$[\text{C}_4\text{MIm}][\text{NTf}_2]$	H–F [%]	H–O [%]
cation	25.5	28.1
anion	30.4	35.1

Obviously, in the $[\text{Al}(\text{hfp})_4]^-$ salt, contacts are mostly created between H and F, whereas in the $[\text{NTf}_2]^-$ salt, also H–O contacts occur to a great extent. Keeping in mind that F atoms in CF_3 groups are hardly polarizable and carry less negative charge than O atoms in the $\text{S}^+–\text{O}^-$ bonds of the $[\text{NTf}_2]^-$ anion, H–F contacts probably account for less interaction energy than H–O contacts. Therefore, $[\text{C}_4\text{MIm}][\text{NTf}_2]$ includes more stronger interactions than $[\text{C}_4\text{MIm}][\text{Al}(\text{hfp})_4]$, which is dominated by weaker H–F interactions. So we can suggest that ions in the $[\text{NTf}_2]^-$ salt tend to have a higher binding energy, and accordingly its ionicity is well below that of the $[\text{Al}(\text{hfp})_4]^-$ salt.

It is clear that for a complete quantitative analysis, one would have to weigh the contacts according to the interatomic distance. For such an analysis, a reference point is necessary, as well as a function describing the energy profile, which lies far beyond the scope of this work.

A modified Marcus ansatz to account for the ion dynamics

To shed even more theoretical light on our results, we now turn to the description of ion-hopping processes in the context of the statistical mechanics of simple models of ILs. They capture the interplay of free volume, through the hard-sphere model, and Coulomb effects represented by point charges underlying many physical and chemical properties of ILs. They provide insight by simple analytical solutions or approximations remarkably close to computer simulations. We note that the subtleties associated with the chemical details can either be dealt with by modifying the ion shape and intraionic charge distributions of the constituents, or by atomically resolved models, both of which require large-scale computer simulations.

To transfer an ion in a polarizable dielectric medium, a charged particle must hop from an occupied donor position to a vacant acceptor region. Whereas the net thermodynamic driving force for this process vanishes, the sheer existence of localized charges requires the presence of an activation barrier. The energetics of the ion-hopping process can be decomposed into two contributions: First, a cavity accommodating the ion must be created in the acceptor region; second, moving the charge from the donor to the acceptor site polarizes the latter and depolarizes the former. Within the so-called restricted primitive model of charged hard spheres of equal diameter d and charge $\pm Ze$, the free energy of creating a cavity is given by the hard-sphere contribution ΔG_{HSF} [Eq. (13)],

$$\Delta G_{\text{HSF}} \cong \Delta F_{\text{HSF}} = \frac{6Vk_{\text{B}}T}{\pi} \left(\frac{3\xi_1\xi_2}{\Delta} + \frac{3\xi_2^3}{\Delta\xi_3} + \frac{3\xi_2^3}{\xi_3^2} \ln \Delta - \xi_0 \ln \Delta \right) \quad (13)$$

where ΔF_{HSF} is the change in Helmholtz free energy of the hard-sphere fluid, $\Delta = 1 - \xi_3$ is the packing fraction of the system and the density dependent coefficients ξ_i are given by Equation (14),

$$\xi_i = \frac{\pi}{6} \rho \sigma^i \quad (14)$$

where σ^i is the hard sphere diameter. Our numerical results do not depend strongly on the use of Equation (13); for example, applying the simulation data of creating a cavity in water leads to a very similar physical picture, as described below. We assume a packing fraction of 0.6 to be typical for liquid ILs. The packing index of IL crystals is around 0.65 close to room temperature.^[53,54] However, on melting it further decreases and reaches values of roughly 0.60. Setting the packing index to higher values would not change the qualitative results at all, and even would only change quantitative results in the range of 5%. Experimentally determined packing indices are included in the Supporting Information.

For the charge contribution, we make use of an expression similar to that given by Marcus for the outer-sphere contribution to electron-transfer processes.^[55,56] This quantity depends

on the amount of charge localized on the donor and acceptor (Z_A and Z_D), their diameter d and their separation R [Eq. (15)]. Note that, in contrast to electronic transport, the ions in ionic transport phenomena do not change their diameter during charge transport. Therefore, only one diameter appears in the equations,

$$\Delta G_{\text{pot}} \cong \Delta F_{\text{pot}} \cong V_{\text{pot}} = -\frac{e^2}{4\pi\epsilon_0} \left(1 - \frac{1}{\epsilon}\right) \left(\frac{Z_D^2}{d} + \frac{Z_A^2}{d} - \frac{Z_A Z_D}{R}\right) \quad (15)$$

where G_{pot} is the Gibbs free energy, F_{pot} is the Helmholtz free energy, and V_{pot} is the potential energy.

We take a typical^[57] IL dielectric constant of $\epsilon = 10$ and a hopping distance of one ionic diameter, and results are again rather insensitive to the choice of these two parameters. In the Marcus picture of a second-order expansion of the free energy, we arrive at the picture of intersecting parabola, each minimum of which corresponds to the localization of an ion at a favorable site (cf. Figures 4 and 5). As a reorganization free enthalpy λ , we have the vertical transfer of an ion from one potential energy to the other without rearranging the ions in the neighborhood of the acceptor. It is given by the sum of ΔG_{HSF} and ΔG_{pot} . It is straightforward to show that the activation barrier of the ion-transfer process is given by $\lambda/4$.

Numerical results for the activation barrier as a function of the hard-sphere diameter are shown in Figure 5. In the region relevant to the anions discussed here, the barriers are slightly less than 1 eV ($\approx 100 \text{ kJ mol}^{-1}$), quite close to the B values in the VFT fits of viscosities and conductivities (see Appendix) multiplied by the Boltzmann constant to convert them to energies (cf. Tables 5 and 6). Up to about 1 nm, the activation barrier decreases with increasing ion diameter. Here, the monotonically decreasing polarization contribution overcompensates the monotonically increasing cavity-formation term. In combination, they give rise to a very shallow curve around the diameters of the ions discussed here.

The diameters of $[\text{Al}(\text{hfp})_4]^-$ and $[\text{NTf}_2]^-$ were calculated from the crystal structures of the $[\text{C}_2\text{MIm}]^+$ salts (CSD refcodes

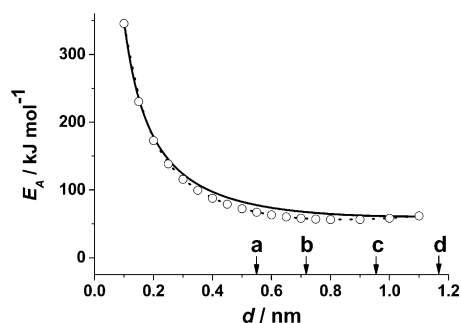


Figure 5. Free activation energies E_A for equisized charged hard spheres as a function of their diameter d . Solid line: hard-sphere contributions based on Equation (13); circles and interpolated dotted line: cavity-formation free energies in water.^[58] The arrows indicate the lateral (a), average (b), and longitudinal (c) diameters of $[\text{NTf}_2]^-$ and the diameter of $[\text{Al}(\text{hfp})_4]^-$ (d).

MALCOT and RENSEJ01) by measuring the mean distance between fluorine and aluminum or fluorine and nitrogen atoms, respectively. Adding the van der Waals diameter of fluorine^[59] gave the diameter of the anions. The $[\text{NTf}_2]^-$ anion is of non-spherical shape and therefore has longitudinal (from F to F) and lateral axes. The latter can be seen as the distance between two adjacent F atoms, between two adjacent O atoms, or a mixture of both. Since we wanted to have a lower and an upper limit for the diameter, we took the (shorter) distance between the O atoms and also added their van der Waals diameter to obtain the lateral diameter. The values are listed in Table 4. The aluminate shows a diameter of slightly more than

Table 4. Anion diameters of $[\text{NTf}_2]^-$ and $[\text{Al}(\text{hfp})_4]^-$ calculated from the crystal structures of their $[\text{C}_2\text{MIm}]^+$ salts and the van der Waals diameters.

anion	longitudinal diameter [nm]	lateral diameter [nm]
$[\text{NTf}_2]^-$	0.950	0.549
$[\text{Al}(\text{hfp})_4]^-$	1.166	

1.1 nm, whereas the imide has a mean diameter of 0.722 nm. As mentioned above, the activation barrier decreases with increasing particle diameter up to approximately 1 nm. $[\text{Al}(\text{hfp})_4]^-$ lies exactly in this ideal region, whereas the $[\text{NTf}_2]^-$ anion appears to be smaller and is further away from the minimum activation energy. Accordingly, $[\text{Al}(\text{hfp})_4]^-$ should be able to change its position more easily and thus show lower viscosities, higher conductivities, and larger diffusion constants. Nevertheless, our results also clearly show that $[\text{NTf}_2]^-$ is a very good anion for the synthesis of good ILs and are therefore in agreement with the vast amount of studies in the last decade concerning $[\text{NTf}_2]^-$ ILs. This conclusion can also be supported by comparing the herein-presented viscosity and conductivity values with, for example, those of $[\text{PF}_6]^-$ salts which have a much smaller anion ($V_m^- = 0.107 \text{ nm}^{3[60]}$). $[\text{C}_4\text{MIm}][\text{PF}_6]$ has a viscosity of 207 mPas at 25 °C^[61] and conductivities of 1.465 mS cm^{-1} at 25 °C and 5.78 mS cm^{-1} at 55 °C.^[62] Both $[\text{C}_4\text{MIm}][\text{NTf}_2]$ (3.16 mS cm^{-1} at 25 °C and 8.22 mS cm^{-1} at 55 °C) and $[\text{C}_4\text{MIm}][\text{Al}(\text{hfp})_4]$ (6.51 mS cm^{-1} at 55 °C) have much higher conductivities, and $[\text{C}_4\text{MIm}][\text{NTf}_2]$ shows a much lower viscosity of 52.3 mPas at 25 °C ($[\text{C}_4\text{MIm}][\text{Al}(\text{hfp})_4]$ is solid at 25 °C). For $[\text{C}_6\text{MIm}]^+$ salts, the differences are even larger: $[\text{C}_6\text{MIm}][\text{PF}_6]$ (0.62 mS cm^{-1} at 25 °C^[63]) cannot compete with $[\text{C}_6\text{MIm}][\text{NTf}_2]$ (2.09 mS cm^{-1}) and $[\text{C}_6\text{MIm}][\text{Al}(\text{hfp})_4]$ (2.36 mS cm^{-1}). Of course, this model, due to its relative simplicity and the diverse chemical nature of different classes of ILs, cannot cover all subtleties. This becomes clear when looking at viscosity and conductivity data of $[\text{BF}_4]^-$ salts, for instance. However, it gives a good explanation of general trends and can shed more light on the behavior of many ionic liquids.

Conclusion

We have investigated the dynamic properties of 24 ILs consisting of imidazolium and ammonium cations as well as $[\text{NTf}_2]^-$

and $[\text{Al}(\text{hfp})_4]^-$ anions with the focus on ion-specific self-diffusion constants and ionicities.

Viscosities and conductivities show a common behavior, which can be described by Arrhenius and VFT equations. Most of the $[\text{Al}(\text{hfp})_4]^-$ ILs are less viscous and more conductive than their $[\text{NTf}_2]^-$ analogues. Additionally, they show a much smaller dependence on the cation, which can be attributed to their spherical shape, larger size, and less polarizable surface.

Ion-specific self-diffusion constants D of the ILs were measured and showed a similar trend to viscosities, that is, $[\text{Al}(\text{hfp})_4]^-$ ILs diffuse faster than $[\text{NTf}_2]^-$ ILs, and imidazolium ILs faster than comparable ammonium ILs. It was possible to describe the ratio D^+/D^- of all $[\text{NTf}_2]^-$ and $[\text{Al}(\text{hfp})_4]^-$ ILs with a single equation, respectively. The equations are a generalized form of the Stokes–Einstein equation, which is not valid here in its original form. The exponents of the equations showed that ions in ILs based on $[\text{Al}(\text{hfp})_4]^-$ anions exhibit less intermolecular interactions than ions in $[\text{NTf}_2]^-$ ILs.

From self-diffusion constants and bulk conductivities, ionicities for most of the ILs could be calculated. It was shown that $[\text{Al}(\text{hfp})_4]^-$ ILs in most cases have higher ionicities than their $[\text{NTf}_2]^-$ analogues, culminating in ionicities of virtually 100%. Furthermore, variation of cations changes ionicities by altering the degree of dispersion interaction and steric effects. These influences, however, are more complex and less predictable. Moreover, due to the interplay of cations and anions, the cation effects differ from anion to anion. Since ionicities can be seen as a measure for the fraction of free ions in a liquid electrolyte, this result means that some $[\text{Al}(\text{hfp})_4]^-$ ILs with short aliphatic side chains ($n \approx 4$) in the cations virtually do not show ion pairing. To our knowledge, this is the first time that ILs almost without ion pairing have been reported.

We used a modified Marcus theory to describe our results quantitatively. With increasing anion diameter, the activation energy for movement of an ion to an empty site decreases up to diameters of more than 1 nm. In this picture, $[\text{Al}(\text{hfp})_4]^-$ has an almost ideal diameter of 1.17 nm, whereas $[\text{NTf}_2]^-$ has a mean diameter of 0.722 nm and therefore a higher activation energy and worse transport properties than $[\text{Al}(\text{hfp})_4]^-$. Altogether, despite its simplicity this model gives a very good description and explanation of the experimental results, but must of course be adapted in individual cases to properties such as ion shape and polarizability. Especially for applications in electrochemical devices, these results can be used to design high-performance IL-based systems.

Appendix

Although for most of the examined ILs, viscosity and conductivity data exist,^[4,38, 63–65] we measured all ILs again on the same device under the same conditions to exclude errors resulting from different setups and to ensure reproducibility and comparability of the data.

Viscosity measurements

VFT fitting parameters of all investigated ILs are listed in Table 5. The experimental data points are included in Figures 1 and 2. The

Table 5. Parameters for the viscosities of $[\text{Al}(\text{hfp})_4]^-$ and $[\text{NTf}_2]^-$ ILs in the VFT Equation [Eq. (4)], determined from the VFT fits in Figure 1. R^2 values were greater than or equal to 0.999 and are not given for each individual entry.

IL	η_0 [mPas]	B [K]	T_0 [K]
$[\text{C}_2\text{MIm}][\text{NTf}_2]$	0.2458	632	169
$[\text{AllylMIm}][\text{NTf}_2]$	0.0659	1009	138
$[\text{C}_4\text{MIm}][\text{NTf}_2]$	0.3336	572	185
$[\text{C}_4\text{MMIm}][\text{NTf}_2]$	0.0559	1061	158
$[\text{C}_6\text{MIm}][\text{NTf}_2]$	0.0590	1014	155
$[\text{C}_8\text{MIm}][\text{NTf}_2]$	0.0241	1324	138
$[\text{C}_{10}\text{MIm}][\text{NTf}_2]$	0.0389	1206	148
$[\text{C}_2\text{MIm}][\text{Al}(\text{hfp})_4]$	0.0040	2402	38
$[\text{AllylMIm}][\text{Al}(\text{hfp})_4]$	0.1066	905	144
$[\text{C}_4\text{MIm}][\text{Al}(\text{hfp})_4]$	0.0430	1130	132
$[\text{C}_4\text{MMIm}][\text{Al}(\text{hfp})_4]$	0.0985	853	157
$[\text{C}_6\text{MIm}][\text{Al}(\text{hfp})_4]$	0.1743	709	170
$[\text{C}_8\text{MIm}][\text{Al}(\text{hfp})_4]$	0.0134	1486	112
$[\text{C}_{10}\text{MIm}][\text{Al}(\text{hfp})_4]$	0.0069	1716	104
$[\text{N}_{1123}][\text{NTf}_2]$	0.0403	1151	147
$[\text{N}_{1444}][\text{NTf}_2]$	0.0061	1601	157
$[\text{N}_{1888}][\text{NTf}_2]$	0.0052	2008	127
$[\text{N}_{2225}][\text{NTf}_2]$	0.0505	1054	169
$[\text{N}_{2666}][\text{NTf}_2]$	0.0036	1756	140
$[\text{N}_{1123}][\text{Al}(\text{hfp})_4]$	0.1219	837	164
$[\text{N}_{1444}][\text{Al}(\text{hfp})_4]$	0.0552	946	163
$[\text{N}_{1888}][\text{Al}(\text{hfp})_4]$	0.0102	1582	125
$[\text{N}_{2225}][\text{Al}(\text{hfp})_4]$	0.0205	1269	142
$[\text{N}_{2666}][\text{Al}(\text{hfp})_4]$	0.0432	1005	163

unusually small T_0 value of the VFT fit for $[\text{C}_2\text{MIm}][\text{Al}(\text{hfp})_4]$ possibly results from the small number of data points and from its generally peculiar behavior (see below). However, the fitting itself was very stable in the case of $[\text{C}_2\text{MIm}][\text{Al}(\text{hfp})_4]$ and yielded the same parameters for a variety of different starting values.

Conductivity measurements

Conductivities of the ILs were measured during heating in the temperature range from room temperature up to 80 °C. Figure 2 shows the results, which were fitted with a VFT ansatz, except for $[\text{C}_6\text{MIm}][\text{Al}(\text{hfp})_4]$ and $[\text{N}_{1123}][\text{Al}(\text{hfp})_4]$. For these ILs, due to unsolvable mathematical instabilities and—in the case of the high-melting $[\text{N}_{1123}][\text{Al}(\text{hfp})_4]$ —few data points, VFT fits could not yield reasonable parameters and an Arrhenius approach was chosen as more applicable in these cases. For all other ILs, R^2 values are always significantly better for VFT fits, and thus VFT fits were used to calculate conductivities at 25 °C (see Ionicities section). Table 6 lists the fit parameters for VFT and Arrhenius fits. In the case of $[\text{C}_4\text{MMIm}][\text{Al}(\text{hfp})_4]$, the data point at 323.15 K was not included in the fit. As with viscosities, $[\text{C}_2\text{MIm}][\text{Al}(\text{hfp})_4]$ again shows very different values of σ_0 and T_0 , which may again be attributed to the limited number of data points as well as to the overall behavior of this IL.

Conductivities follow analogous trends to viscosities: The smaller the cation, the more conductive the IL. $[\text{Al}(\text{hfp})_4]^-$ ILs are more conductive than $[\text{NTf}_2]^-$ ILs, again with the exceptions of the small $[\text{C}_2\text{MIm}]^+$ and $[\text{N}_{1123}]^+$ cations.

Nomenclature

Ammonium cations are abbreviated as $[\text{N}_{abcd}]^+$, and 1-methyl-3-*n*-alkylimidazolium cations as $[\text{C}_n\text{MIm}]^+$. The indices *a*, *b*, *c*, *d*, and *n* describe the number of carbon atoms of the *n*-alkyl chains at-

Table 6. Parameters for the conductivities of $[\text{Al}(\text{hflp})_4]^+$ and $[\text{NTf}_2]^-$ ILs in the VFT equation [Eq. (6)], determined from the VFT fits in Figure 2. $[\text{C}_6\text{MIm}][\text{Al}(\text{hflp})_4]$ and $[\text{N}_{1123}][\text{Al}(\text{hflp})_4]$ could only be fitted sensibly with an Arrhenius approach [Eq. (5)].

IL	σ_0 [mS cm^{-1}]	B [K]	T_0 [K]
$[\text{C}_2\text{MIm}][\text{NTf}_2]$	174.8	301	204
$[\text{AllylMIm}][\text{NTf}_2]$	1024.6	769	144.0
$[\text{C}_4\text{MIm}][\text{NTf}_2]$	267.6	481	190
$[\text{C}_6\text{MMIm}][\text{NTf}_2]$	1110.4	857	163
$[\text{C}_8\text{MIm}][\text{NTf}_2]$	345.6	588	183
$[\text{C}_8\text{MIm}][\text{NTf}_2]$	316.7	622	186
$[\text{C}_{10}\text{MIm}][\text{NTf}_2]$	398.1	773	173
$[\text{C}_2\text{MIm}][\text{Al}(\text{hflp})_4]$	1000.2	1258	68
$[\text{AllylMIm}][\text{Al}(\text{hflp})_4]$	93.1	241	220
$[\text{C}_4\text{MIm}][\text{Al}(\text{hflp})_4]$	37.89	113	264
$[\text{C}_4\text{MMIm}][\text{Al}(\text{hflp})_4]$	558.4	425.6	144.6
$[\text{C}_6\text{MIm}][\text{Al}(\text{hflp})_4]$	31 989 ^[a]	23.65 ^[a]	
$[\text{C}_8\text{MIm}][\text{Al}(\text{hflp})_4]$	154.2	537	181
$[\text{C}_{10}\text{MIm}][\text{Al}(\text{hflp})_4]$	294.2	796	152
$[\text{N}_{1123}][\text{NTf}_2]$	2038	1120	128
$[\text{N}_{1444}][\text{NTf}_2]$	1536	1060	176
$[\text{N}_{1888}][\text{NTf}_2]$	181.5	901	188
$[\text{N}_{2225}][\text{NTf}_2]$	772.6	809	177
$[\text{N}_{2666}][\text{NTf}_2]$	546.0	1050	169
$[\text{N}_{1123}][\text{Al}(\text{hflp})_4]$	9994.4 ^[a]	20.46 ^[a]	
$[\text{N}_{1444}][\text{Al}(\text{hflp})_4]$	259.3	713	167
$[\text{N}_{1888}][\text{Al}(\text{hflp})_4]$	377.1	1020	155
$[\text{N}_{2225}][\text{Al}(\text{hflp})_4]$	115.8	430	199
$[\text{N}_{2666}][\text{Al}(\text{hflp})_4]$	315.7	868	165

[a] Since VFT fits did not converge to reasonable values, Arrhenius parameters σ_0 [in mS cm^{-1}] and A [in kJ mol^{-1}] are given.

tached to the N atom. Exceptions are 1-allyl-3-methylimidazolium and 1-butyl-2,3-dimethylimidazolium, which are abbreviated as $[\text{AllylMIm}]^+$ and $[\text{C}_4\text{MMIm}]^+$, respectively. Further abbreviations are as follows: hflp = hexafluoroisopropoxy, Tf = trifluoromethanesulfonate.

Acknowledgements

We would like to thank the Deutsche Forschungsgemeinschaft (SPP1191 "Ionic Liquids" and "WCACaps" project) for financial support. A. Rupp wishes to thank the Fonds der Chemischen Industrie for financial support.

Keywords: ion pairs · ionic liquids · Marcus theory · transport properties · weakly coordinating anions

- [1] H. Weingärtner, *Angew. Chem.* **2008**, *120*, 664–682; *Angew. Chem. Int. Ed.* **2008**, *47*, 654–670.
- [2] R. D. Rogers, K. R. Seddon, *Science* **2003**, *302*, 792–793.
- [3] I. Raabe, K. Wagner, K. Guttsche, M. Wang, M. Grätzel, G. Santiso-Quinones, I. Krossing, *Chem. Eur. J.* **2009**, *15*, 1966–1976.
- [4] S. Bulut, P. Klose, M.-M. Huang, H. Weingärtner, P. J. Dyson, G. Laurenczy, C. Friedrich, J. Menz, K. Kümmerer, I. Krossing, *Chem. Eur. J.* **2010**, *16*, 13139–13154.
- [5] P. Wasserscheid and T. Welton, *Ionic Liquids in Synthesis*, Wiley-VCH, Weinheim, **2008**.
- [6] D. Wei, T. W. Ng, *Electrochem. Commun.* **2009**, *11*, 1996–1999.
- [7] J. L. Anderson, J. K. Dixon, J. F. Brennecke, *Acc. Chem. Res.* **2007**, *40*, 1208–1216.

- [8] O. Hollóczki, D. Gerhard, K. Massone, L. Szarvas, B. Nemeth, T. Veszpremi, L. Nyulaszi, *New J. Chem.* **2010**, *34*, 3004–3009.
- [9] X. Han, D. W. Armstrong, *Acc. Chem. Res.* **2007**, *40*, 1079–1086.
- [10] G. B. Appetecchi, M. Montanari, M. Carewska, M. Moreno, F. Alessandrini, S. Passerini, *Electrochim. Acta* **2011**, *56*, 1300–1307.
- [11] C. Arbizzani, M. Biso, D. Cericola, M. Lazzari, F. Soavi, M. Mastragostino, *J. Power Sources* **2008**, *185*, 1575–1579.
- [12] A. Balducci, F. Soavi, M. Mastragostino, *Appl. Phys. A: Mater. Sci. Process.* **2006**, *82*, 627–632.
- [13] M. Diaw, A. Chagnes, B. Carré, P. Willmann, D. Lemordant, *J. Power Sources* **2005**, *146*, 682–684.
- [14] S. Passerini, F. Alessandrini, G. B. Appetecchi, M. Conte, *ECS Trans.* **2006**, *1*, 67–71.
- [15] F. Wu, R. Chen, F. Wu, L. Li, B. Xu, S. Chen, G. Wang, *J. Power Sources* **2008**, *184*, 402–407.
- [16] D. R. MacFarlane, M. Forsyth, P. C. Howlett, J. M. Pringle, J. Sun, G. Annat, W. Neil, E. I. Izgorodina, *Acc. Chem. Res.* **2007**, *40*, 1165–1173.
- [17] K. R. Seddon, *Nat. Mater.* **2003**, *2*, 363–365.
- [18] W. Xu, E. I. Cooper, C. A. Angell, *J. Phys. Chem. B* **2003**, *107*, 6170–6178.
- [19] M.-M. Huang, S. Bulut, I. Krossing, H. Weingärtner, *J. Chem. Phys.* **2010**, *133*, 101101.
- [20] A. W. Taylor, P. Licence, A. P. Abbott, *PhysChemComm PhysChemChem-Phys* **2011**, *13*, 10147–10154.
- [21] P. Walden, *Z. Phys. Chem. (Leipzig)*, **1906**, *55*, 207–246.
- [22] P. Walden, *Z. Phys. Chem. (Leipzig)*, **1906**, *55*, 246.
- [23] H. Rodriguez, J. F. Brennecke, *J. Chem. Eng. Data* **2006**, *51*, 2145.
- [24] O. O. Okoturo, T. J. VanderNoot, *J. Electroanal. Chem.* **2004**, *568*, 167.
- [25] H. Tokuda, K. Hayamizu, K. Ishii, M. A. B. H. Susan, M. J. Watanabe, *J. Phys. Chem. B* **2005**, *109*, 6103–6110.
- [26] J. Jacquemin, P. Husson, A. A. H. Padua, V. Majer, *Green Chem.* **2006**, *8*, 172.
- [27] K. Ueno, H. Tokuda, M. Watanabe, *Phys. Chem. Chem. Phys.* **2010**, *12*, 1649–1658.
- [28] D. R. MacFarlane, P. Meakin, J. Sun, N. Amini, M. Forsyth, *J. Phys. Chem. B* **1999**, *103*, 4164–4170.
- [29] H. Matsumoto, T. Mazda, Y. Miyazaki, *Chem. Lett.* **2000**, *29*, 1430–1431.
- [30] A. P. Abbott, *ChemPhysChem* **2004**, *5*, 1242–1246.
- [31] U. Preiss, S. Bulut, I. Krossing, *J. Phys. Chem. B* **2010**, *114*, 11133–11140.
- [32] U. P. R. M. Preiss, J. M. Slattery, I. Krossing, *Ind. Eng. Chem. Res.* **2009**, *48*, 2290–2296.
- [33] E. O. Stejskal, J. E. Tanner, *J. Chem. Phys.* **1965**, *42*, 288–292.
- [34] T. Umecky, M. Kanakubo, Y. Ikushima, *Fluid Phase Equilib.* **2005**, *228–229*, 329–333.
- [35] S. Seki, K. Hayamizu, S. Tsuzuki, K. Fujii, Y. Umebayashi, T. Mitsugi, T. Kobayashi, Y. Ohno, Y. Kobayashi, Y. Mita, H. Miyashiro, S.-i. Ishiguro, *Phys. Chem. Chem. Phys.* **2009**, *11*, 3509–3514.
- [36] H. Liu, E. Maginn, A. E. Visser, N. J. Bridges, E. B. Fox, *Ind. Eng. Chem. Res.* **2012**, *51*, 7242–7254.
- [37] A. Noda, K. Hayamizu, M. Watanabe, *J. Phys. Chem. B* **2001**, *105*, 4603–4610.
- [38] B. Garcia, S. Lavallee, G. Perron, C. Michot, M. Armand, *Electrochim. Acta* **2004**, *49*, 4583–4588.
- [39] H. Tokuda, S. Tsuzuki, M. A. B. H. Susan, K. Hayamizu, M. Watanabe, *J. Phys. Chem. B* **2006**, *110*, 19593–19600.
- [40] G. Annat, D. R. MacFarlane, M. Forsyth, *J. Phys. Chem. B* **2007**, *111*, 9018–9024.
- [41] O. Borodin, W. Gorecki, G. D. Smith, M. Armand, *J. Phys. Chem. B* **2010**, *114*, 6786–6798.
- [42] T.-Y. Wu, I.-W. Sun, S.-T. Gung, M.-W. Lin, B.-K. Chen, H. P. Wang, S.-G. Su, *J. Taiwan Inst. Chem. Eng.* **2011**, *42*, 513–522.
- [43] K. R. Harris, M. Kanakubo, *Faraday Discuss.* **2012**, *154*, 425–438.
- [44] H. Matsumoto, H. Sakaebe, K. Tatsumi, *J. Power Sources* **2005**, *146*, 45–50.
- [45] S. Tsuzuki, *ChemPhysChem* **2012**, *13*, 1664–1670.
- [46] S. Zahn, G. Bruns, J. Thar, B. Kirchner, *Phys. Chem. Chem. Phys.* **2008**, *10*, 6921–6924.
- [47] K. Fumino, A. Wulf, R. Ludwig, *Angew. Chem.* **2008**, *120*, 8859–8862; *Angew. Chem. Int. Ed.* **2008**, *47*, 8731–8734.
- [48] P. A. Hunt, *J. Phys. Chem. B* **2007**, *111*, 4844–4853.
- [49] H. Tokuda, K. Hayamizu, K. Ishii, M. A. B. H. Susan, M. Watanabe, *J. Phys. Chem. B* **2004**, *108*, 16593–16600.

- [50] F. L. Hirshfeld, *Theor. Chim. Acta* **1977**, *44*, 129–138.
- [51] M. A. Spackman, D. Jayatilaka, *CrystEngComm* **2009**, *11*, 19–32.
- [52] J. J. McKinnon, M. A. Spackman, A. S. Mitchell, *Acta Crystallogr. Sect. B: Structural Sci.* **2004**, *60*, 627–668.
- [53] W. Beichel, P. Eiden, I. Krossing, *ChemPhysChem* **2013**, *14*, 3221–3226.
- [54] W. Beichel in *From the Crystal Structures of Organic Salts to Consistent Ion Volumes and their Charge Distribution*, Thesis, Albert-Ludwigs-Universität, Freiburg, **2013**.
- [55] R. A. Marcus, *J. Chem. Phys.* **1956**, *24*, 966–978.
- [56] R. A. Marcus, *J. Chem. Phys.* **1956**, *24*, 979–989.
- [57] H. Weingärtner, *Zeitschr. Physik. Chem.* **2006**, *220*, 1395–1405.
- [58] T. C. Beutler, D. R. Beguelin, W. F. van Gunsteren, *J. Chem. Phys.* **1995**, *102*, 3787–3793.
- [59] M. Mantina, A. C. Chamberlin, R. Valero, C. J. Cramer, D. G. Truhlar, *J. Phys. Chem. A* **2009**, *113*, 5806–5812.
- [60] C. Ye, J. n. M. Shreeve, *J. Chem. Phys. A* **2007**, *111*, 1456–1461.
- [61] C. Frez, G. J. Diebold, C. D. Tran, S. Yu, *J. Chem. Eng. Data* **2006**, *51*, 1250–1255.
- [62] O. Zech, A. Stoppa, R. Buchner, W. Kunz, *J. Chem. Eng. Data*, **2010**, *55*, 1774–1778.
- [63] K. Nakamura, T. Shikata, *ChemPhysChem* **2010**, *11*, 285–294.
- [64] S. Bulut in *Novel Ionic Liquids with Weakly Coordinating Anions: Synthesis Characterization, Principal Physical Properties and Their Predictions*, Thesis, Albert-Ludwigs-Universität, Freiburg, **2010**.
- [65] M. Tariq, P. J. Carvalho, J. A. P. Coutinho, I. M. Marrucho, J. N. C. Lopes, L. P. N. Rebelo, *Fluid Phase Equilib.* **2011**, *301*, 22–32.

Received: January 15, 2014
Published online on July 10, 2014